DALTON
FULL PAPER

Lanthanide complexes of a new sterically hindered potentially hexadentate podand ligand based on a tris(pyrazolyl)borate core; crystal structures, solution structures and luminescence properties

Zoe R. Reeves,[a] Karen L. V. Mann,[a] John C. Jeffery,[a] Jon A. McCleverty,*[a] Michael D. Ward,*[a] Francesco Barigelletti[b] and Nicola Armaroli *[b]

[a] *School of Chemistry, University of Bristol, Cantock's Close, Bristol, UK BS8 1TS. E-mail: mike.ward@bristol.ac.uk*
[b] *Istituto FRAE–CNR, Via P. Gobetti 101, 40129 Bologna, Italy*

Received 9th November 1998, Accepted 14th December 1998

The new podand ligand hydrotris[3-(6-methyl)pyridin-2-ylpyrazol-1-yl]borate $[L^1]^-$ was prepared which contains three bidentate pyrazolyl/pyridine arms attached to a $\{BH\}^-$ head-group. This ligand differs from an earlier ligand hydrotris[3-(2-pyridyl)pyrazol-1-yl]borate $[L^2]^-$ by the presence of methyl groups attached to the C^6 positions of the pyridyl rings, which would interfere with each other sterically if the ligand co-ordinated in a fully hexadentate manner. Instead, crystallographic analysis of the complexes $[M(L^1)(NO_3)_2(H_2O)]$ (M = Eu, Tb or Gd) showed that partial dissociation of the podand occurs to relieve this potential steric problem: either one or two of the pyridyl groups are not co-ordinated, such that $[L^1]^-$ is penta- or tetra-dentate, but instead are involved in intramolecular N ··· H–O hydrogen-bonding interactions with the co-ordinated water molecule. The presence of both structural forms in single crystals of the gadolinium and europium complexes shows that interconversion between them in solution must be facile. Variable-temperature ^{1}H NMR spectra of the diamagnetic lanthanum(III) analogue shows that, whereas all three ligand arms are equivalent on the NMR timescale at high temperatures, at −80 °C there is mirror symmetry in the complex such that two arms are equivalent and the third is different from the other two; this is consistent with the crystalline form in which $[L^1]^-$ is tetradentate with two pendant pyridyl arms, which has pseudo-mirror symmetry. Luminescence studies showed that whereas the ligand-based luminescence is retained in the gadolinium(III) complex, in the europium(III) and terbium(III) complexes the ligand-centred emission is quenched by ligand-to-metal energy transfer, resulting in the usual metal-centred emission spectra. The intensity of the emission from the europium(III) and terbium(III) complexes of $[L^1]^-$ is substantially reduced compared to the emission from the analogous complexes $[M(L^2)(NO_3)_2]$ (M = Eu or Tb) which we ascribe to the sterically induced poorer co-ordination of the podand ligand, resulting in (i) less efficient ligand-to-metal energy transfer, and (ii) co-ordination of labile solvent molecules (H_2O) to the metal centres.

Introduction

The study of lanthanide complexes has attracted much attention because of their important practical applications.[1,2] In particular Eu^{3+} and Tb^{3+} are characterised by long-lived (ms timescale) and strongly luminescent electronically excited states, which makes them appealing for analytical purposes, especially in the biomedical field.[1,3,4] However in order to exploit this luminescence, the lanthanide ion must be co-ordinated to a suitable multidentate ligand in order to: (i) populate the lanthanide emitting level taking advantage of a large ligand absorption cross section, followed by ligand-to-metal energy transfer, because the lanthanide f–f excited states are not readily accessible by direct excitation; and (ii) protect the ion co-ordination sphere from solvent interactions, which can deactivate its excited state *via* non-radiative processes.[3] Several research groups have put much effort into designing well tailored ligands, and a great variety of them are now available.[4–12] In general, one can say that small variations in a ligand structure can lead to remarkable changes in the photophysical properties. So far, our contribution in the field has been the synthesis and characterisation of some podand ligands based on the tris(pyrazolyl)borate core;[13] in particular we have described the photophysical properties of a tris[3-(2-pyridyl)pyrazol-1-yl]-hydroborate] $[L^2]^-$ (Chart 1) and its 1 : 1 and 1 : 2 complexes $[Ln(L^2)(NO_3)_2]$ and $[Ln(L^2)_2]^+$, where Ln indicates Eu^{3+}, Tb^{3+}, or Gd^{3+}.[14] Interestingly, $[Tb(L^2)(NO_3)_2]$ (hereafter abbreviated Tb**2**) is soluble and stable in polar (H_2O, MeOH) and apolar (CH_2Cl_2) solvents, displaying in each case high emission quantum yields, namely 0.13 in water and 0.38 in MeOH. Here we report the photophysical characterisation of the new ligand L^1 and its 1 : 1 complexes $[Ln(L^1)(NO_3)_2(H_2O)]$ (abbreviated Ln**1**; Ln = La, Eu, Gd or Tb), where L^1 differs from L^2 by the presence of a methyl substituent at the C^6 position on each pyridyl group. Relatively minor changes in the degree of steric crowding at the solvent co-ordination site can in some cases have a significant affect on the accessibility of solvent molecules to these sites and on their exchange rate,[15] which could in turn strongly affect luminescence properties. Accordingly we were interested to see whether this apparently small modification of the parent ligand L^2 would lead to significant differences in the structural and spectroscopic properties of the lanthanide complexes.

Experimental

The following instruments were used for routine spectroscopic analysis: NMR spectra (^{1}H and ^{11}B), a JEOL Lambda 300 spectrometer; electron-impact (EI) and fast-atom bombardment (FAB) mass spectra, a VG-Autospec instrument; IR spectra, a Perkin-Elmer FT-1600 spectrometer. 2-Bromo-6-methylpyridine was prepared according to the published method.[16]

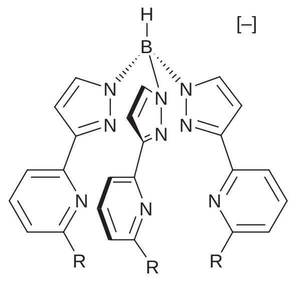

$[L^1]^-$ R = Me (series **1** complexes)
$[L^2]^-$ R = H (series **2** complexes)

Chart 1

Preparations

2-Acetyl-6-methylpyridine (A). This preparation is based on a published method.[17] To a solution of 2-bromo-6-methylpyridine (10.0 g, 0.058 mol) in thf (200 cm^3) at −78 °C under N_2 was added slowly *n*-butyllithium (1.6 M solution in hexanes: 36 cm^3, 0.058 mol). After this a solution of *N*,*N*-dimethylacetamide (5.56 g, 0.064 mol) in diethyl ether (50 cm^3) was added dropwise whilst maintaining cooling at −78 °C. This resulted in a deep orange mixture which was allowed to warm to −10 °C and hydrolysed with HCl (6 M, 40 cm^3). The solvent was removed under reduced pressure and the residual oil was made basic with aqueous sodium hydroxide. The crude product was extracted with several portions of CH_2Cl_2, and the combined organic extracts were washed with water and dried ($MgSO_4$). Purification by vacuum distillation (*ca.* 90 °C, 2 mm Hg) afforded the product as a pale yellow oil (6.98 g, 88%). EIMS: *m*/*z* 135 (M^+). ^1H NMR (300 MHz, $CDCl_3$): δ 2.58 (3 H, s, CH_3), 2.67 (3 H, s, CH_3), 7.27 (1 H, d, $J = 7.7$; H^3 or H^5), 7.66 (1 H, t, $J = 7.7$; H^4) and 7.78 (1 H, d, $J = 7.7$ Hz; H^5 or H^3).

3-Dimethylamino-1-(6-methylpyridin-2-yl)prop-2-en-1-one (B). A mixture of the above product **A** (10.0 g, 0.074 mol) and dimethylformamide dimethyl acetal (20 cm^3) was heated to reflux for 10 h, yielding a dark brown solution. After cooling, the excess of dimethylformamide dimethyl acetal was removed *in vacuo* to leave a brown oil. Prolonged drying under vacuum afforded a solid which was recrystallised from $CHCl_3$–hexane to give **B** as a yellow crystalline solid (8.44 g, 60%). EIMS: *m*/*z* 190 (M^+). ^1H NMR (300 MHz, $CDCl_3$): δ 2.75 (3 H, s, CH_3), 3.07 (3 H, s, NCH_3), 3.19 (3 H, s, NCH_3), 6.61 (1 H, d, $J = 12$, C*H*=CH), 7.31 (1 H, d, $J = 7.8$; pyridyl H^3 or H^5), 7.80 (1 H, t, $J = 7.8$; pyridyl H^4), 7.94 (1 H, d, $J = 12$; CH=C*H*) and 8.02 (1 H, d, $J = 7.8$ Hz; pyridyl H^5 or H^3). IR (KBr disc): ν_{CO} 1638 cm^{-1} (Found: C, 69.6; H, 7.5; N, 14.7. $C_{11}H_{14}N_2O$ requires: C, 69.5; H, 7.4; N, 14.7%).

3-(6-Methyl)pyridin-2-yl-1*H*-pyrazole (C). A mixture of compound **B** (10.0 g, 0.053 mol) and hydrazine monohydrate (15 cm^3) in ethanol (30 cm^3) was heated to reflux for 30 min. After removal of the solvents under reduced pressure the solid residue was recrystallised from $CHCl_3$–hexane to give pure **C** (7.56 g, 92%). EIMS: *m*/*z* 159 (M^+). ^1H NMR (300 MHz, $CDCl_3$): δ 2.60 (3 H, s; CH_3), 6.79 (1 H, d, $J = 2$; pyrazolyl H^4 or H^5), 7.09 (1 H, d, $J = 7.5$; pyridyl H^3 or H^5), 7.53 (1 H, d, $J = 7.8$; pyridyl H^5 or H^3), 7.64 [2 H, m; pyridyl H^4 and pyrazolyl (H^5 or H^4)] (Found: C, 68.0; H, 5.8; N, 26.2. C_3H_3N requires: C, 67.9; H, 5.7; N, 26.4%).

Potassium hydrotris[3-(6-methyl)pyridin-2-ylpyrazol-1-yl]-borate (KL^1). A mixture of compound **C** (2.00 g, 12.6 mmol) and KBH_4 (0.17 g, 3.1 mol) was ground to ensure intimate mixing and was then heated to 200 °C for 1 h, during which the mixture melted. The melt was cooled and toluene (*ca.* 40 cm^3) added and the mixture stirred at room temperature for 2 h. The solution was filtered, and hexane added to the filtrate to induce precipitation of a white solid. This was filtered off and recrystallised from CH_2Cl_2–hexane to yield a white crystalline solid (0.72 g, 43%). This compound is predominantly the desired product (≈85% by ^{11}B NMR: see Results and discussion section) but also contains some of the bis(pyrazolyl)-borate and tetrakis(pyrazolyl)borate analogues. Further recrystallisation resulted in a purer compound but reduced the yield (*ca.* 30%). Negative-ion FABMS: *m*/*z* 486 $\{[L^1]^-\}$. IR (KBr disc): ν_{B-H} 2390 cm^{-1} (Found: C, 61.8; H, 4.3; N, 22.8. $C_{27}H_{25}BKN_9$ requires: C, 61.6; H, 4.8; N, 24.0%).

Complexes $[M(L^1)(NO_3)_2(H_2O)]$ (M = Eu, Gd, Tb or La). A solution of the appropriate lanthanide(III) nitrate hydrate (0.1 mmol) and KL^1 (0.053 g, 0.1 mmol) in the minimum amount of methanol (*ca.* 3 cm^3) was stirred at room temperature to afford a precipitate that was collected by filtration, washed and dried. Yields of complexes were in the range 30–60%. Crystals were grown by allowing hexane to diffuse into a concentrated solution of the complexes in CH_2Cl_2. Analytical and mass spectroscopic data for the complexes are collected in Table 1. ^1H NMR data for $[La(L^1)(NO_3)_2(H_2O)]$ (CD_2Cl_2, 300 MHz): δ 7.82 (1 H, d, $J = 2.2$; pyrazolyl H^4 or H^5), 7.68 (1 H, t, $J = 7.8$; pyridyl H^4), 7.47 (1 H, d, $J = 7.8$; pyridyl H^3 or H^5), 7.15 (1 H, d, $J = 7.8$; pyridyl H^5 or H^3), 6.59 (1 H, d, $J = 2.2$ Hz; pyrazolyl H^5 or H^4) and 2.70 (3 H, s; CH_3).

X-Ray crystallography

Suitable crystals were quickly transferred from the mother-liquor to a stream of cold N_2 on a Siemens SMART diffractometer fitted with a CCD-type area detector. In all cases a full sphere of data was collected at −100 °C using graphite-monochromatised Mo-Kα radiation. A detailed experimental description of the methods used for data collection and integration using the SMART system has been published.[13] Table 2 contains a summary of the crystal parameters, data collection and refinement. The absorption correction was applied using SADABS.[18] In all cases the structures were solved by conventional direct methods and refined by the full-matrix least-squares method on all F^2 data using the SHELXTL 5.03 package on a Silicon Graphics Indy computer.[19] Non-hydrogen atoms were refined with anisotropic thermal parameters; hydrogen atoms were included in calculated positions and refined with isotropic thermal parameters riding on those of the parent atom.

None of the structural determinations presented any particular problems. In $[Tb(L^1)(NO_3)_2(H_2O)]\cdot CH_2Cl_2$ the molecule of CH_2Cl_2 is disordered with one of the Cl atoms [Cl(1)] being disordered over two closely spaced sites (site occupancies 0.67 and 0.33). Although it is reasonable to assume that the second Cl atom should be similarly disordered, Cl(2) actually refined successfully without being split and has a reasonable isotropic thermal parameter. The maximum residual electron-density peak is close to this disordered solvent molecule. The complexes $[Eu(L^1)(NO_3)_2(H_2O)]$ and $[Gd(L^1)(NO_3)_2(H_2O)]$ are isostructural and isomorphous, and both contain two independent molecules in the asymmetric unit which have substantially different conformations (see Results and discussion). The maximum residual electron-density peaks are close to the metal ion in both cases.

CCDC reference number 186/1281.

See http://www.rsc.org/suppdata/dt/1999/349/ for crystallographic files in .cif format.

Photophysical studies

The solvent used for the photophysical investigations was spectrofluorimetric grade CH_2Cl_2 (Carlo Erba). Absorption spectra were recorded with a Perkin-Elmer Lambda 5 spectrophotometer. Emission and excitation spectra were obtained with a Spex Fluorolog II spectrofluorimeter, equipped with a

Hamamatsu R-928 photomultiplier tube. Fluorescence quantum yields were measured with the method described by Demas and Crosby[20] using as standards $[Ru(bipy)_3]Cl_2$ (bipy = 2,2′-bipyridine; $\Phi = 0.028$ in aerated water)[21] for the Eu^{3+} complex, and quinine sulfate ($\Phi = 0.546$ in 0.5 mol dm^{-3} H_2SO_4)[22] for the Tb^{3+} complex. The luminescence decays were recorded by using a pulsed xenon lamp as excitation source (Spex 1934D phosphorimeter) and elaborated with current software fitting procedures (Origin 3.78). Comparisons of luminescence lifetimes in the presence of water and D_2O were performed with a Perkin-Elmer LS-50B spectrofluorimeter according to a previously published method.[13]

Results and discussion

Ligand synthesis

The synthesis of the new ligand $[L^1]^-$ (as its potassium salt) is summarised in Scheme 1, and essentially follows the method used for the preparation of the unsubstituted analogue $[L^2]^-$. Conversion of 2-bromo-6-methylpyridine into 2-acetyl-6-methylpyridine (**A**) was effected in high yield by a known general method.[17] The two-step conversion of the acetyl group into a pyrazole (**C**) *via* the intermediate dimethylamino-substituted enone (**B**) likewise is a standard route which works easily and with good yields.[13,23]

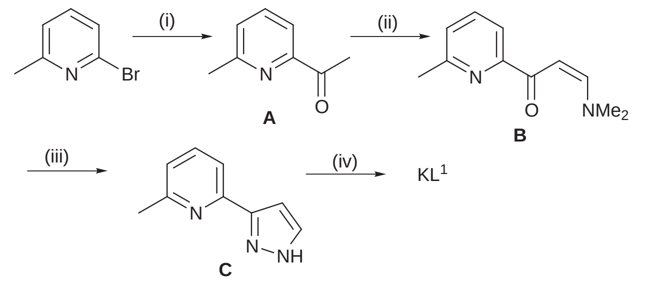

Scheme 1 (i) BuLi, *N*,*N*-dimethylacetamide; (ii) *N*,*N*-dimethylformamide dimethyl acetal; (iii) hydrazine hydrate, ethanol; (iv) KBH_4, melt.

The preparation of KL^1 involved reaction of compound **C** with KBH_4 in a melt at 200 °C according to the usual method for preparing tris(pyrazolyl)borates. We found it necessary in this case to optimise the conditions carefully to avoid excessive contamination of the product with the bis(pyrazolyl)borate and tetrakis(pyrazolyl)borate analogues, which arise from reaction of two or four equivalents of **C** respectively with the KBH_4. A 3:1 **C**:KBH_4 ratio resulted in significant amounts of the bis(pyrazolyl)borate in the product, so the proportion of **C** was increased to about 4:1; beyond this, significant quantities of the tetrakis(pyrazolyl)borate were produced. The constitution of the product mixture was most easily checked by ^{11}B NMR spectra in CD_3OD. The desired tris(pyrazolyl)borate has its ^{11}B resonance at δ −2.8, whereas the bis- and tetrakis-(pyrazolyl)borate contaminants have their ^{11}B resonances at δ −8.2 and +1.1 respectively. We were able to obtain after one recrystallisation of the product a material which was about 85% pure; further recrystallisations substantially reduced the yield but gave purer material. Characterisation of KL^1 was on the basis of a negative-ion FAB mass spectrum in which the most intense peak corresponded to $[L^1]^-$.

Table 1 Analytical and mass spectroscopic data for the new complexes

Complex	Analysis (%) C	H	N	FABMS[b] M^+, *m*/*z*
$[Tb(L^1)(NO_3)_2(H_2O)]$	40.9 (41.2)	3.4 (3.4)	19.3 (19.6)	707
$[Gd(L^1)(NO_3)_2(H_2O)]$	41.4 (41.3)	3.2 (3.4)	18.8 (19.6)	706
$[Eu(L^1)(NO_3)_2(H_2O)]$	42.0 (41.5)	3.8 (3.5)	19.3 (19.7)	701
$[La(L^1)(NO_3)_2(H_2O)]$	41.0 (40.8)	3.3 (3.5)	18.9 (19.0)[c]	687

[a] Expected values in parentheses. [b] The molecular ions in the FAB mass spectra all correspond exactly to loss of one nitrate ion and water from the complex, giving $\{M(L^1)(NO_3)\}^+$. [c] Expected values based on 0.5 CH_2Cl_2 per complex molecule.

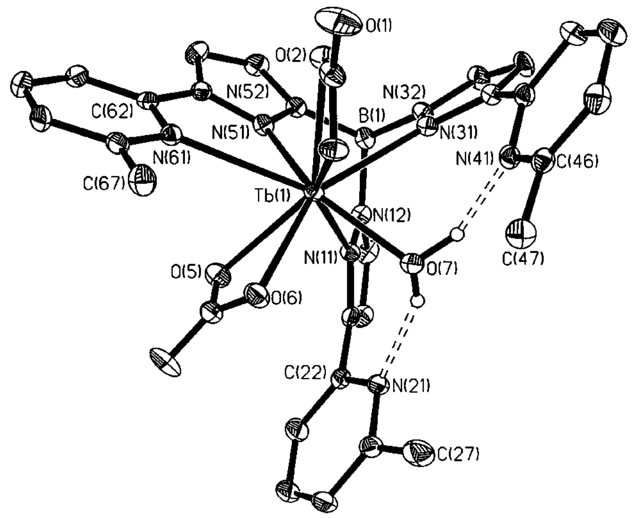

Fig. 1 Crystal structure of $[Tb(L^1)(NO_3)_2(H_2O)]$.

Syntheses and crystal structures of lanthanide complexes

Reaction of KL^1 with lanthanide(III) nitrate salts (Eu, Gd, Tb) in MeOH using a 1:1 ligand:metal ratio afforded precipitates of the complexes. FAB Mass spectrometry and elemental analyses confirmed the 1:1 ligand:metal ratio, and X-ray crystallographic analyses showed the complexes to be of the form $[M(L^1)(NO_3)_2(H_2O)]$, hereafter abbreviated as Eu**1**, Tb**1**, *etc.*

The structure of complex Tb**1** is in Fig. 1; selected bond lengths are given in Table 3. The metal ion is nine-co-ordinate, from four nitrogen donors of the ligand L^1 (all three pyrazolyl rings and one pyridyl ring), two bidentate nitrate ligands and a co-ordinated water molecule. The two non-co-ordinated pyridyl residues of L^1 are involved in hydrogen-bonding interactions with the protons of the co-ordinated water molecule: the non-bonded N(21)···O(7) and N(41)···O(7) distances are 2.696(4) and 2.632(4) Å respectively, indicative of strong O–H···N hydrogen-bonding interactions.[24] In order to optimise this hydrogen bonding these two pyridyl rings are twisted away from the planes of the co-ordinated pyrazolyl rings to which they are attached; the dihedral twists are 46 and 31° for the pyridyl rings containing N(21) and N(41) respectively. It is noticeable that for the two ligand arms whose pyridyl groups are twisted away from the metal ion, the Tb–N (pyrazolyl) distances are likewise stretched [Tb(1)–N(11) 2.590, Tb–N(31) 2.644 Å] compared to that of the genuinely bidentate arm [Tb(1)–N(51) 2.392 Å].

Comparison of this structure with those of the complexes with $[L^2]^-$ (Ln**2**; Ln = Eu, Er or Pr) shows that the methyl substituents at the pyridyl C^6 positions have a substantial effect on the structure. In these complexes with $[L^2]^-$ all six donors of the ligand are co-ordinated together with two nitrates to give 10-co-ordinate lanthanide ions, with all three bidentate arms showing similar co-ordination behaviour such that the three M–N (pyrazolyl) distances are similar to one another, and likewise the three M–N (pyridyl) distances are similar to one another. Co-ordination of $[L^1]^-$ in the same way would result in steric interference between the methyl substituents on the pyridyl rings, which would be directed towards one another. This problem is alleviated by partial dissociation of $[L^1]^-$, in particular rotation of two of the pyridyl rings away from the plane of the pyrazolyl rings to which they are attached, such that these pyridyl residues are not co-ordinated, and consequently the associated metal–pyrazolyl bonds are also lengthened. This creates sufficient space in the metal ion co-ordination sphere for a water molecule to co-ordinate, and this water ligand is neatly stabilised by hydrogen bonds to the two pendant pyridyl rings. Such 'second-sphere' stabilisation of a co-ordinated H_2O ligand by hydrogen bonding with pendant fragments of a larger multidentate ligand has been observed before, in $[Cu(L^2)(H_2O)][PF_6]$.[25]

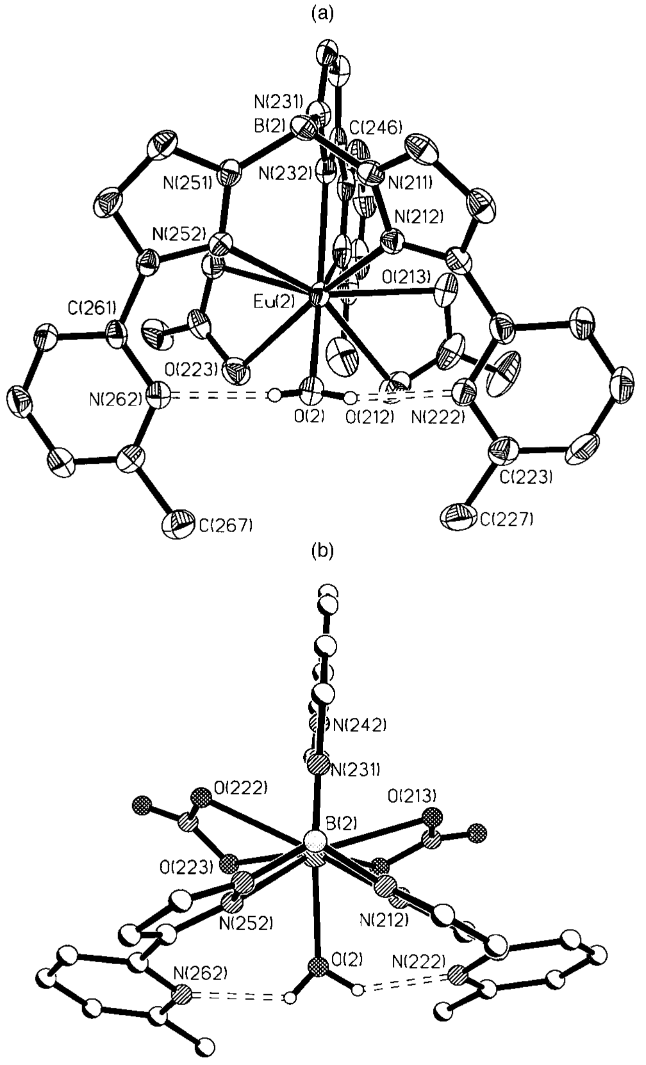

Fig. 2 Two views of one of the independent complex units in the crystal structure of $[Eu(L^1)(NO_3)_2(H_2O)]$ (the gadolinium analogue is essentially identical).

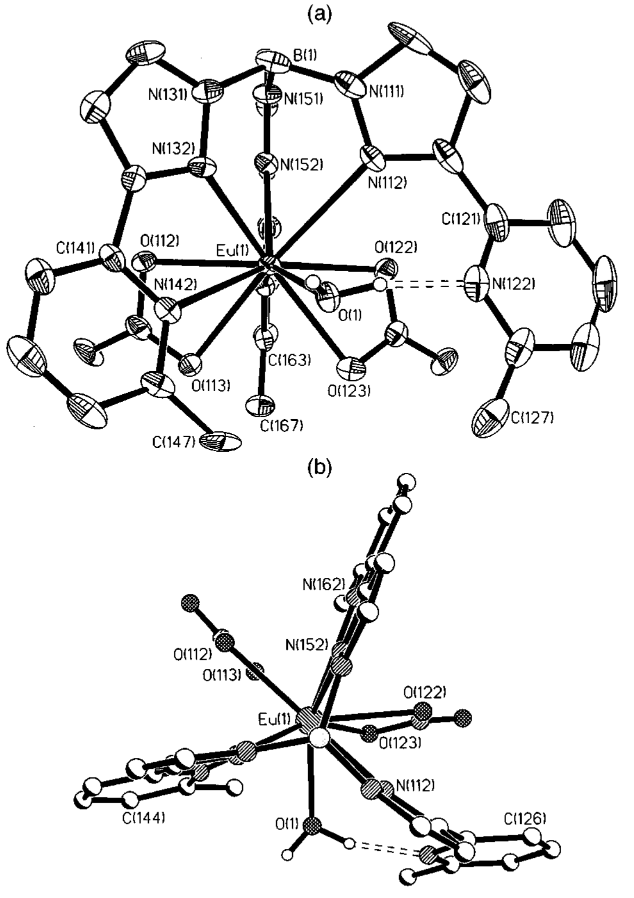

Fig. 3 Two views of the second independent complex unit in the crystal structure of $[Eu(L^1)(NO_3)_2(H_2O)]$ (the gadolinium analogue is essentially identical).

Table 2 Crystallographic data for the three structures[a]

	$[Tb(L^1)(NO_3)_2(H_2O)]\cdot CH_2Cl_2$	$[Eu(L^1)(NO_3)_2(H_2O)]$	$[Gd(L^1)(NO_3)_2(H_2O)]$
Formula	$C_{28}H_{29}BCl_2N_{11}O_7Tb$	$C_{27}H_{27}BEuN_{11}O_7$	$C_{27}H_{27}BGdN_{11}O_7$
M	872.25	780.37	785.65
System, space group	Monoclinic, $P2_1/c$	Triclinic, $P\bar{1}$	Triclinic, $P\bar{1}$
a/Å	18.588(2)	10.876(3)	10.870(2)
b/Å	16.3820(12)	16.507(5)	16.4827(13)
c/Å	11.3938(14)	19.011(6)	18.996(2)
α/°		70.302(5)	70.356(7)
β/°	106.099(7)	82.212(5)	82.054(8)
γ/°		73.796(7)	73.900(13)
U/Å^3	3333.4(6)	3082(2)	3076.0(6)
Z	4	4	4
D_c/g cm^{-3}	1.738	1.682	1.697
μ/mm^{-1}	2.345	2.099	2.221
Crystal size/mm	0.38 × 0.12 × 0.10	0.24 × 0.18 × 0.04	0.20 × 0.20 × 0.30
Reflections collected: total, independent, R_{int}	20996, 7578, 0.0333	27838, 13136, 0.0555	31882, 13905, 0.0207
Data, restraints, parameters	7578, 0, 472	13136, 6, 865	13905, 0, 853
Final $R1$, $wR2^{b,c}$	0.0259, 0.0591	0.0453, 0.0856	0.0226, 0.0579
Weighting factors[c]	0.0272, 0	0.0275, 0	0.0334, 0
Largest residuals/e Å^{-3}	+0.438, −1.281	+1.649, −1.209	+1.621, −0.907

[a] Details in common: Mo-Kα radiation (0.71073 Å); temperature for data collection, 173(2) K; 2θ limit for data collected, 55°. [b] Structure was refined on F_o^2 using all data; the value of R_1 is given for comparison with older refinements based on F_o with a typical threshold of $F \geq 4\sigma(F)$. [c] $wR2 = [\Sigma w(F_o^2 - F_c^2)^2/\Sigma w(F_o^2)^2]^{\frac{1}{2}}$ where $w^{-1} = [\sigma^2(F_o^2) + (aP)^2 + bP]$ and $P = [\max(F_o^2, 0) + 2F_c^2]/3$.

Table 3 Selected bond lengths (Å) for the three crystal structures

$[Tb(L^1)(NO_3)_2(H_2O)]\cdot CH_2Cl_2$		$[Eu(L^1)(NO_3)_2(H_2O)]$		$[Gd(L^1)(NO_3)_2(H_2O)]$	
Tb(1)–O(7)	2.296(2)	Eu(2)–O(2)	2.349(4)	Gd(2)–O(191)	2.339(2)
Tb(1)–O(2)	2.506(2)	Eu(2)–O(213)	2.463(4)	Gd(2)–O(183)	2.463(2)
Tb(1)–O(3)	2.436(2)	Eu(2)–O(212)	2.474(4)	Gd(2)–O(184)	2.452(2)
Tb(1)–O(6)	2.447(2)	Eu(2)–O(222)	2.469(4)	Gd(2)–O(173)	2.470(2)
Tb(1)–O(5)	2.482(2)	Eu(2)–O(223)	2.479(4)	Gd(2)–O(174)	2.464(2)
Tb(1)–N(11)	2.590(2)	Eu(2)–N(212)	2.619(5)	Gd(2)–N(111)	2.621(2)
Tb(1)–N(31)	2.644(2)	Eu(2)–N(232)	2.435(5)	Gd(2)–N(131)	2.424(2)
Tb(1)–N(51)	2.392(2)	Eu(2)–N(252)	2.633(4)	Gd(2)–N(151)	2.607(2)
Tb(1)–N(61)	2.780(2)	Eu(2)–N(242)	2.807(5)	Gd(2)–N(141)	2.786(2)
		Eu(1)–O(1)	2.400(3)	Gd(1)–O(91)	2.380(2)
		Eu(1)–O(113)	2.505(4)	Gd(1)–O(83)	2.490(2)
		Eu(1)–O(112)	2.508(4)	Gd(1)–O(84)	2.501(2)
		Eu(1)–O(122)	2.496(4)	Gd(1)–O(73)	2.486(2)
		Eu(1)–O(123)	2.516(4)	Gd(1)–O(74)	2.518(2)
		Eu(1)–N(112)	2.796(5)	Gd(1)–N(51)	2.792(2)
		Eu(1)–N(132)	2.474(4)	Gd(1)–N(11)	2.471(2)
		Eu(1)–N(152)	2.481(4)	Gd(1)–N(31)	2.468(2)
		Eu(1)–N(142)	2.743(4)	Gd(1)–N(41)	2.744(2)
		Eu(1)–N(162)	2.974(4)	Gd(1)–N(21)	2.974(2)

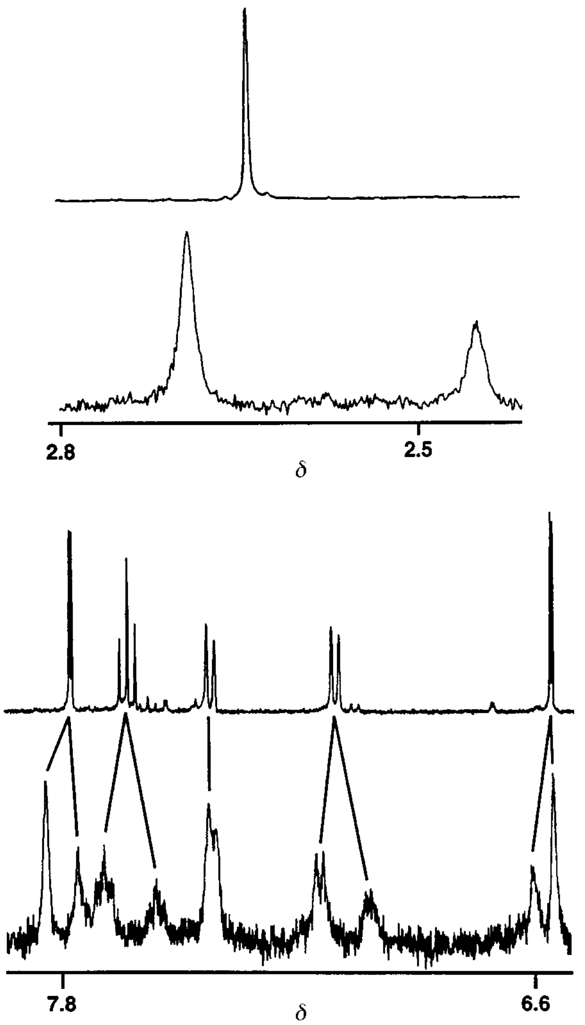

Fig. 4 Proton NMR spectra of $[La(L^1)(NO_3)_2(H_2O)]$ at 20 °C (upper) and −80 °C (lower).

The crystal structures of complexes Eu**1** and Gd**1**, which are isostructural and isomorphous, are particularly interesting as they give insight into the nature of the fluxional behaviour of the molecules in solution, something which is not normally possible for a static crystal structure (Figs. 2 and 3; Table 3). There are two crystallographically independent molecules in the asymmetric unit. One of these is essentially identical to the terbium(III) complex described above, with a nine-co-ordinate metal centre and $[L^1]^-$ being tetradentate with two pendant pyridyl groups hydrogen bonding to a co-ordinated water molecule and two of the M–N (pyrazolyl) bonds significantly longer than the other two. The non-bonded O···N separations for the hydrogen-bonding interactions are as follows: in the europium structure O(2)···N(222) 2.750(6) Å and O(2)···N(262) 2.729(6) Å, with twists between the pyrazolyl and pyridine rings of 42 and 39° respectively; in the gadolinium structure O(191)···N(121) 2.723(4) and O(191)···N(161) 2.755(4) Å, with twists between the pyrazolyl and pyridine rings of 40 and 42° respectively. In the second independent complex unit however $[L^1]^-$ is pentadentate, the metal centre is 10-co-ordinate, and there is only one pendant pyridyl group hydrogen bonded to the water ligand. As we saw before, for the ligand arm whose pyridyl group is pendant, the M–N (pyrazolyl) bond [Eu(1)–N(112) and Gd(1)–N(51)] is also stretched by about 0.25 Å compared to the two bidentate arms. In the europium complex the O(1)···N(122) separation in the hydrogen bond is 2.633(6) Å, with the dihedral twist between the pyridyl and pyrazolyl rings being 44°; the corresponding values for the gadolinium complex are 2.622(4) Å and 44° respectively. The presence of both forms in the crystal structure implies that in solution there is a dynamic process in which one of the pyridyl rings alternates between a co-ordinative interaction with the metal centre and a hydrogen-bonding interaction with the adjacent water ligand. The rearrangement required is minimal: a rotation of *ca.* 40° of the plane of the pyridyl ring about the bond between the pyridyl and pyrazolyl rings, and an associated lengthening of the M–N (pyrazolyl) bond, is sufficient to interconvert the two forms. The balance between electronic effects (which will electrostatically favour co-ordination of the pyridyl group to the hard metal ion) and steric effects (which will favour the lower co-ordination number to relieve overcrowding) is clearly finely balanced.

In order to examine this in more detail we prepared the (diamagnetic) complex La**1** and performed a variable-temperature ^1H NMR study in CD_2Cl_2 (Fig. 4). At room temperature the spectrum is consistent with the molecule having threefold symmetry such that all three arms are equivalent, with a single signal (relative intensity 3 H) for the methyl protons at δ 2.7 and five signals (relative intensity 1H each) in the aromatic region corresponding to the two pyrazolyl and three pyridyl protons. This means that all three pyrazolylpyridine arms take their turn to be bidentate (fully co-ordinated) or monodentate with a pendant pyridyl ring, and that the water and nitrate ligands

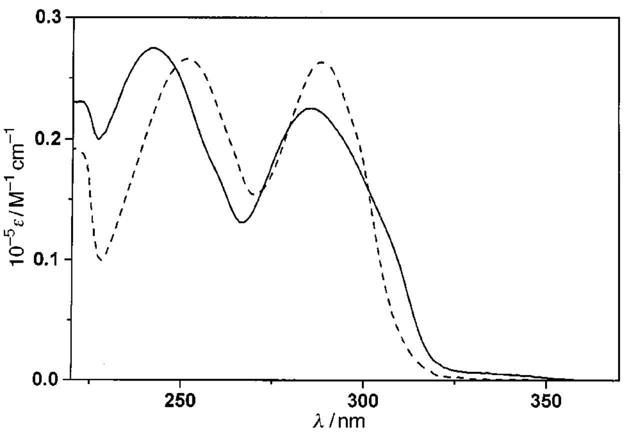

Fig. 5 Absorption spectra of K[L^1] (– – –) and [Tb(L^1)$(NO_3)_2(H_2O)$] (——) in CH_2Cl_2 solution at room temperature.

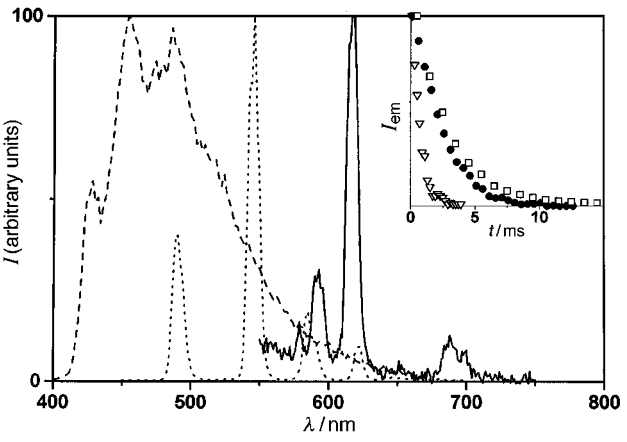

Fig. 6 Emission spectra of [Gd(L^1)$(NO_3)_2(H_2O)$] (– – –) in a CH_2Cl_2 rigid matrix at 77 K, [Tb(L^1)$(NO_3)_2(H_2O)$] (······) and [Eu(L^1)-$(NO_3)_2(H_2O)$] (——) in CH_2Cl_2 at 298 K. In the inset are shown the corresponding luminescence decays: Gd (square), Tb (dark circle), Eu (triangle).

exchange positions. On cooling the spectrum starts to broaden at −40 °C, is very broad and indistinct at −60 °C, and by −80 °C has resolved into two sets of signals in a 2 : 1 ratio: thus, there are two methyl signals at δ 2.5 (one methyl group) and 2.8 (two methyl groups), and the same splitting into two sets of signals is apparent in four of the five aromatic resonances. At this temperature the fluxional motion is therefore frozen out and the complex molecule adopts a co-ordination mode in which one arm is different from the other two. Examination of Fig. 2 shows that this structure could correspond to the crystallographically characterised conformer in which the water ligand hydrogen bonds to two pyridyl groups, as there is an approximate (non-crystallographic) plane of symmetry passing through the fully co-ordinated bidentate arm, the boron atom, the metal atom, and the oxygen atom of the water ligand. In contrast the alternative crystallographically characterised conformer, with one pendant pyridyl group involved in hydrogen bonding, cannot have twofold symmetry.

To conclude this section, we can say that: The effect of the methyl substituents is to prevent for steric reasons full hexadentate co-ordination of the podand [L^1]$^-$. Instead, complete dissociation of one or two pyridyl ligands occurs together with substantial lengthening of the related M–N (pyrazolyl) bonds, making room in the co-ordination sphere for a water ligand which becomes involved in intramolecular hydrogen bonding with the pendant pyridyl group(s). There is a fluxional process in solution which interconverts the co-ordinated and pendant pyridyl groups. Whilst this results in apparent threefold symmetry at high temperatures, in the low-temperature limit the structure has mirror symmetry with two of the ligand arms being monodentate and involved in hydrogen bonding to the water ligand, and the third arm being fully co-ordinated.

Photophysical properties of the ligand and its europium(III) and terbium(III) complexes

Unlike the complexes Ln**2** (Ln = Eu, Tb or Gd) which were stable in a variety of solvents,[14] the new complexes Ln**1** are thermally stable only in dichloromethane. In MeOH the absorption spectra of the complexes tend to change within a few minutes, indicating partial decomplexation, which is understandable in view of the relatively weak co-ordination of [L^1]$^-$ that is apparent from the crystal structures. In water the complexes are practically insoluble. Consequently, our photophysical investigations were carried out in CH_2Cl_2 solution.

The free ligand [L^1]$^-$, as its potassium salt, displays intense absorption bands in the UV spectral region at 252 (ε = 26600) and 288 nm (ε = 26300 dm^3 mol^{-1} cm^{-1}) (Fig. 5). These bands, as expected,[14] are strongly perturbed upon complexation of a lanthanide(III) ion. In Fig. 5 the absorption spectrum of Tb**1** is also reported; Eu**1** and Gd**1** display almost identical spectral profiles.

Free [L^1]$^-$ exhibits an intense, short-lived UV fluorescence in CH_2Cl_2 solution (λ_{max} = 338 nm, Φ_{em} = 0.027, τ < 1 ns) which, in a rigid matrix at 77 K, is accompanied by a strong, long-lived, and structured phosphorescence band (λ_{max} = 462 nm, τ = 800 ms). These emissions are due to the deactivation of the lowest electronic excited singlet and triplet states respectively. Like the 'free' ligand, Gd**1** displays ligand-centred (LC) fluorescence both at room temperature (λ_{max} = 336 nm, Φ_{em} = 0.005, τ < 1 ns) and at 77 K, and LC phosphorescence at 77 K only (λ_{max} = 456 nm, τ = 2.6 ms), Fig. 6. This is an expected result since the metal centred (MC) electronic levels of Gd^{3+} are known to be located at 31000 cm^{-1},[26] typically well above the ligand-centred electronic levels of aromatic ligands. Therefore, ligand-to-metal energy transfer and the consequent MC luminescence cannot be observed as happens, in contrast, for Tb^{3+} and Eu^{3+} complexes. The lower fluorescence quantum yield and the shorter phosphorescence lifetime exhibited by complex Gd**1** compared to free [L^1]$^-$ indicate that the heavy ion facilitates intersystem crossing processes. From the highest energy phosphorescence feature of Gd**1** the position of the lowest ligand-centred excited triplet state is estimated to be about 23400 cm^{-1}, and this value can be taken also for the Eu^{3+} and Tb^{3+} analogues.

The ligand-centred luminescence is completely quenched in complexes Eu**1** and Tb**1**; instead, excitation of ligand-centred absorption bands results in the typical narrow emission bands of the Eu^{3+} and Tb^{3+} ions (Fig. 6). The excitation spectra of both complexes match the corresponding absorption profiles throughout the UV spectral region, showing that ligand-to-metal energy transfer occurs. Interestingly, the emission quantum yields of Tb**1** and Eu**1** in CH_2Cl_2 (0.22 and 0.0001 respectively) are much lower than those of Tb**2** and Eu**2** (0.41 and 0.050, respectively), although the two ligands are only slightly structurally different. In particular, Eu**1** is very weakly luminescent, and its spectrum is barely detectable over the instrumental noise (Fig. 6); the corresponding lifetime is also very short, *i.e.* 0.62 ms *vs.* 1.7 ms for Eu**2**. This weakening of the luminescence is evident, albeit less dramatically, for Tb**1** (Φ_{em} = 0.22) in comparison with Tb**2**, while the lifetimes are identical in the two cases (2.0 ms). The principal quenching mechanism of the luminescent excited state of Tb^{3+} complexes is thermally activated back energy transfer to the ligand-centred triplet level,[3] but this cannot account for the reduced emission quantum yield of Tb**1** compared to Tb**2** because the energy of this ligand-centred triplet state (about 24000 cm^{-1}, see above) is almost identical for both ligands [L^1]$^-$ and [L^2]$^-$. Similarly, the principal mechanism for deactivation of the luminescent

Eu^{3+} excited state (conversion into a non-emissive LMCT excited state)[3] cannot account for the dramatic decrease of luminescence in Eu**1** relative to Eu**2**, because $[L^1]^-$ and $[L^2]^-$ should have very similar electron-donor properties.

Based on their crystal structures, we ascribe the relatively weak luminescence of complexes Eu**1** and Tb**1** to (i) the incomplete co-ordination of the podand ligand, and (ii) the greater accessibility of the metal ion to solvent molecules, both arising from the steric effects of the methyl groups on the pyridyl rings. Incomplete co-ordination of the podand will result in less efficient ligand-to-metal energy transfer after excitation than in the complexes with $[L^2]^-$, and therefore less likelihood of the luminescent excited state being populated; and the presence of co-ordinated OH oscillators from the water ligand provides an additional effective route for quenching.[3,27]

The effect of the co-ordinated water on luminescence quenching was checked by comparing the emission lifetimes of complexes Eu**1** and Tb**1** in CH_2Cl_2 before and after shaking with D_2O, which will result in exchange of any (labile) H_2O ligands by D_2O. In both cases a noticeable increase in the luminescence lifetime was observed after treatment with D_2O, and use of the Horrocks equations gave values for q (the number of co-ordinated water molecules) of 0.8 for Eu**1** and 1.0 for Tb**1**.[1,3,13,27] These are the same within the limits of accuracy of the method, and are consistent with the presence of one water molecule being co-ordinated to each metal centre in CH_2Cl_2 solution, in agreement with both the crystallographic and low-temperature NMR results.

It is clear that a relatively modest change in the ligand structure can give dramatic variations in the luminescence properties of the corresponding lanthanide complexes, which in turn suggests that the search for ligands which exactly optimise the useful properties of lanthanide complexes is still a challenging task.

Acknowledgements

We thank the EPSRC (UK) and the Italian National Research Council (CNR) for financial support. We also thank M. Minghetti for technical assistance, and Dr Rowena Paul for the variable-temperature NMR spectra.

References

1 D. Parker and J. A. G. Williams, *J. Chem. Soc.*, *Dalton Trans.*, 1996, 3613.
2 S. Aime, M. Botta, M. Fasano and E. Terreno, *Chem. Soc. Rev.*, 1998, **27**, 19.
3 N. Sabbatini, M. Guardigli and J.-M. Lehn, *Coord. Chem. Rev.*, 1993, **123**, 201.
4 N. Sabbatini, M. Guardigli and I. Manet, in *Handbook on The Physics and Chemistry of Rare Earths*, eds. K. A. Gschneidner Jr. and L. Eyring, Elsevier, Amsterdam, 1996, vol. 23.
5 B. Alpha, R. Ballardini, V. Balzani, J.-M. Lehn, S. Perathoner and N. Sabbatini, *Photochem. Photobiol.*, 1990, **52**, 299.
6 L. Prodi, M. Maestri, R. Ziessel and V. Balzani, *Inorg. Chem.*, 1991, **30**, 3798.
7 S. L. Wu and DeW. Horrocks Jr., *J. Chem. Soc.*, *Dalton Trans.*, 1997, 1497.
8 A. P. de Silva, H. Q. N. Gunaratne, T. E. Rice and S. Steward, *Chem. Commun.*, 1997, 1891.
9 M. P. O. Wolbers, F. C. J. M. van Veggel, B. H. M. Snellink-Ruël, J. W. Hofstraat, F. A. J. Geurts and D. N. Reinhoudt, *J. Am. Chem. Soc.*, 1997, **119**, 138.
10 N. Sabbatini, A. Casnati, C. Fischer, R. Girardini, M. Guardigli, I. Manet, G. Sarti and R. Ungaro, *Inorg. Chim. Acta*, 1996, **252**, 19; G. Ulrich, R. Ziessel, I. Manet, M. Guardigli, N. Sabbatini, F. Fraternali and G. Wipff, *Chem. Eur J.*, 1997, **3**, 1815.
11 N. Martin, J.-C. G. Bünzli, V. McKee, C. Piguet and G. Hopfgartner, *Inorg. Chem.*, 1998, **37**, 577.
12 M. Lata, H. Takalo, V.-M. Mukkala and J. Kankare, *Inorg. Chim. Acta*, 1998, **267**, 63.
13 P. L. Jones, A. J. Amoroso, J. C. Jeffery, J. A. McCleverty, E. Psillakis, L. H. Rees and M. D. Ward, *Inorg. Chem.*, 1997, **36**, 10.
14 N. Armaroli, V. Balzani, F. Barigelletti, M. D. Ward and J. A. McCleverty, *Chem. Phys. Lett.*, 1997, **276**, 435.
15 D. Pubanz, G. González, D. H. Powell and A. E. Merbach, *Inorg. Chem.*, 1995, **34**, 4447.
16 Z. Wang, J. Reibenspies, R. J. Motekaitis and A. E. Martell, *J. Chem. Soc.*, *Dalton Trans.*, 1995, 1511.
17 J. E. Parks, B. E. Wagner and R. H. Holm, *J. Organomet. Chem.*, 1973, **56**, 53.
18 SADABS, A program for absorption correction with the Siemens SMART area-detector system, G. M. Sheldrick, University of Göttingen, 1996.
19 SHELXTL 5.03 program system, Siemens Analytical X-Ray Instruments, Madison, WI, 1995.
20 J. N. Demas and G. A. Crosby, *J. Phys. Chem.*, 1971, **93**, 2841.
21 K. Nakamaru, *Bull. Soc. Chem. Jpn.*, 1982, **5**, 2697.
22 S. R. Meech and D. J. Philips, *J. Photochem.*, 1983, **23**, 193.
23 Y. Lin and S. A. Lang, Jr., *J. Heterocycl. Chem.*, 1977, **14**, 345.
24 A. Novak, *Struct. Bonding* (*Berlin*), 1974, **18**, 177.
25 D. A. Bardwell, J. C. Jeffery, P. L. Jones, J. A. McCleverty and M. D. Ward, *J. Chem. Soc.*, *Dalton Trans.*, 1995, 2921.
26 R. Reisfeld and C. K. Jørgensen, *Lasers and Excited States of Rare Earths*, Springer, Berlin, 1977.
27 W. D. Horrocks and D. R. Sudnick, *Acc. Chem. Res.*, 1981, **14**, 384.

Paper 8/08724E